Marker-independent identification of glioma-initiating cells

Virginie Clément[1], Denis Marino[1], Cristina Cudalbu[2], Marie-France Hamou[3], Vladimir Mlynarik[2], Nicolas de Tribolet[1], Pierre-Yves Dietrich[4], Rolf Gruetter[2], Monika E Hegi[3] & Ivan Radovanovic[1]

Tumor-initiating cells with stem cell properties are believed to sustain the growth of gliomas, but proposed markers such as CD133 cannot be used to identify these cells with sufficient specificity. We report an alternative isolation method purely based on phenotypic qualities of glioma-initiating cells (GICs), avoiding the use of molecular markers. We exploited intrinsic autofluorescence properties and a distinctive morphology to isolate a subpopulation of cells (FL1$^+$) from human glioma or glioma cultures. FL1$^+$ cells are capable of self-renewal *in vitro*, tumorigenesis *in vivo* and preferentially express stem cell genes. The FL1$^+$ phenotype did not correlate with the expression of proposed GIC markers. Our data propose an alternative approach to investigate tumor-initiating potential in gliomas and to advance the development of new therapies and diagnostics.

Human gliomas are primary neoplasms of the central nervous system that grow diffusely, show different grades of local aggressiveness and display histological and immunohistochemical features of glial lineages or less differentiated neural progenitor cells[1–3]. Although the exact cellular origin of gliomas remains unclear[2,3], it has been proposed that only a fraction of cancer cells with stem cell properties, usually named cancer stem cells, has true tumorigenic potential and constitutes a discrete reservoir of glioma-initiating cells[4,5]. Glioma-initiating cells initially had been identified as CD133$^+$ cells[6,7], but recent studies demonstrate a relative lack of specificity of this marker[8–11]. Also, some studies have questioned the existence of a cellular hierarchy dominated by cancer stem cells in solid tumors or alternatively have shed doubt on their supposed rarity[12,13]. Despite current controversies, there is general agreement that tumors are heterogeneous populations of cells, some of which have a superior tumor initiating and propagating ability. There is therefore a need for reliable methods to identify, isolate and characterize the entire glioma-initiating cell reservoir, even if all cells in this set do not necessarily have bona fide stem cell properties or express homogenous molecular markers.

Here we show that the combination of a distinct morphology and autofluorescence emission can be used to identify a subpopulation of glioma cells with self-renewal ability *in vitro* and tumor- initiating and propagating capacity *in vivo*. Cells in this population have enhanced proliferative activity and preferentially express stem cell–related genes. By avoiding the use of molecular markers and relying on general phenotypic properties correlating with tumorigenicity, our results offer a simple approach for identifying glioma-initiating cells that might be efficiently exploited to understand the molecular mechanisms governing tumor growth.

RESULTS

Identification of a new glioma cell subpopulation

A subpopulation of human glioma cells displays autofluorescence emission around 520 nm (in the FL1 channel) upon laser excitation at 488 nm (**Supplementary Table 1** and **Supplementary Fig. 1**). Cells in this fraction, hereafter called FL1$^+$, can be detected both by fluorescence-activated cell sorting (FACS) or fluorescence microscopy in glioma cell cultures and in freshly dissociated glioma tissue (**Fig. 1a–d** and **Supplementary Tables 2–4**). All tumors are labeled according to their type and World Health Organization (WHO) grade and numbered as described in **Supplementary Table 2**. The microscopic analysis of FL1$^+$ cells confirmed that they were large agranular cells with a very high nuclear:cytoplasmic ratio (**Fig. 1c**) correlating with the high forward scatter and a low side scatter in the FACS analysis. In serum-free conditions (stem cell culture conditions), glioma cells form floating colonies enriched in glioma-initiating cells (gliomaspheres)[14]. Analysis of gliomasphere cultures from different tumors showed varying percentages of FL1$^+$ cells (**Supplementary Table 3**, $n = 10$ cultures), which remained stable over 20 passages *in vitro* (**Supplementary Fig. 2**). Analysis of freshly dissociated human gliomas of different malignancy grade and subtype also revealed the presence of a relatively rare FL1$^+$ cell population (**Fig. 1c** and **Supplementary Table 4**; $n = 26$ tissues) displaying on average lower fluorescence intensity (mean of intensity $< 10^2$) than

[1]Division of Neurosurgery, Geneva University Hospitals and University of Geneva, Geneva, Switzerland. [2]Laboratory of Functional and Metabolic Imaging, Ecole Polytechnique Federale de Lausanne, Lausanne, Switzerland. [3]Laboratory of Brain Tumor Biology and Genetics, Department of Neurosurgery, University Hospital Lausanne and University of Lausanne, Lausanne, Switzerland. [4]Department of Oncology, Geneva University Hospitals and University of Geneva, Geneva, Switzerland. Correspondence should be addressed to I.R. (ivan.radovanovic@hcuge.ch).

RECEIVED 8 SEPTEMBER 2009; ACCEPTED 5 JANUARY 2010; PUBLISHED ONLINE 21 FEBRUARY 2010; DOI:10.1038/NMETH.1430

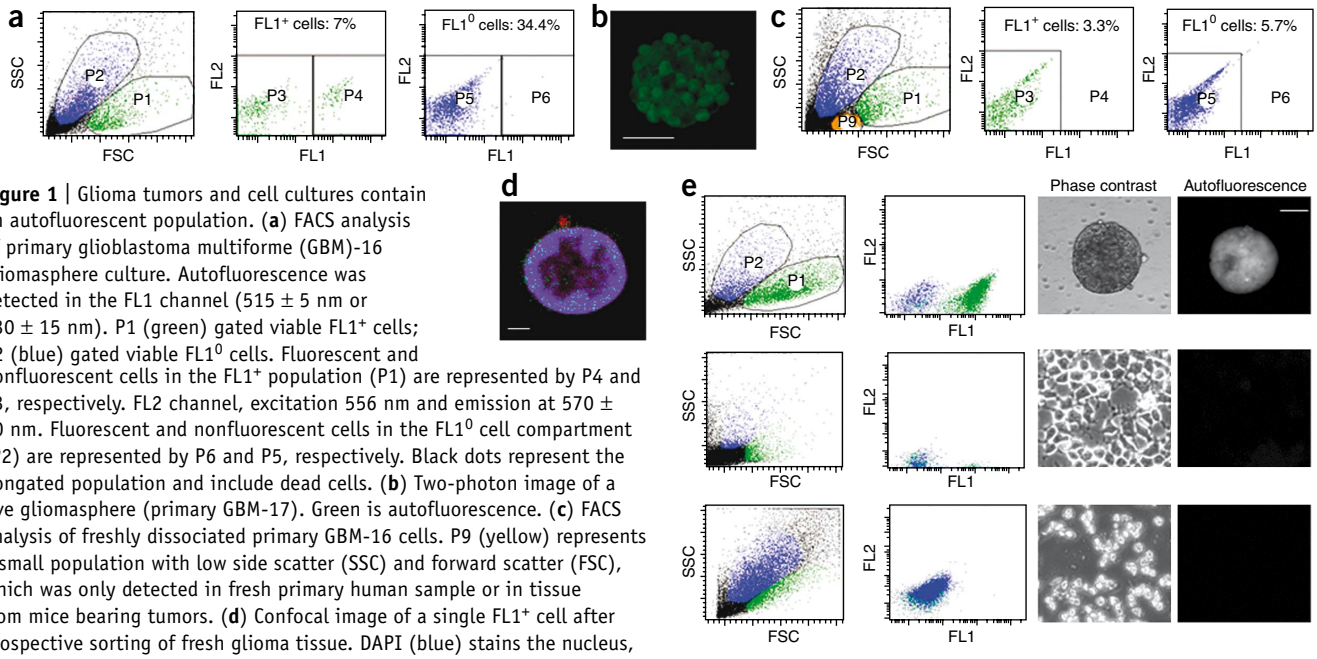

Figure 1 | Glioma tumors and cell cultures contain an autofluorescent population. (**a**) FACS analysis of primary glioblastoma multiforme (GBM)-16 gliomasphere culture. Autofluorescence was detected in the FL1 channel (515 ± 5 nm or 530 ± 15 nm). P1 (green) gated viable FL1$^+$ cells; P2 (blue) gated viable FL1^0 cells. Fluorescent and nonfluorescent cells in the FL1$^+$ population (P1) are represented by P4 and P3, respectively. FL2 channel, excitation 556 nm and emission at 570 ± 10 nm. Fluorescent and nonfluorescent cells in the FL1^0 cell compartment (P2) are represented by P6 and P5, respectively. Black dots represent the nongated population and include dead cells. (**b**) Two-photon image of a live gliomasphere (primary GBM-17). Green is autofluorescence. (**c**) FACS analysis of freshly dissociated primary GBM-16 cells. P9 (yellow) represents a small population with low side scatter (SSC) and forward scatter (FSC), which was only detected in fresh primary human sample or in tissue from mice bearing tumors. (**d**) Confocal image of a single FL1$^+$ cell after prospective sorting of fresh glioma tissue. DAPI (blue) stains the nucleus, and green shows autofluorescence. (**e**) FACS analysis of secondary GBM-1 cells cultured in stem cell medium (top), plated in differentiation medium (middle), and subsequently transfered into stem cell medium to test for 'reversiblity' (bottom). Scale bars, 50 μm (**b**,**e**) and 7.5 μm (**d**).

that observed in gliomasphere cultures (mean of intensity > 10^2). As freshly dissociated cells from tumors were more heterogeneous than cells from gliomasphere cultures, for isolation of FL1$^+$ cells from fresh tissue we adjusted the FACS gating, taking into account cell size, granularity and fluorescence according to the characteristics of the gliomasphere FL1$^+$ population.

Differentiation conditions affect FL1$^+$ cells

Induction of differentiation in gliomaspheres results in cellular changes including cell adherence and expression of neural differentiation markers[4,14–16]. When plated under differentiation conditions (serum-rich medium), purified FL1$^+$ cells and viable nonfluorescent (FL1^0) cells expressed a similar pattern of differentiation markers such as TUJ1, MAP2, GFAP and NESTIN (**Supplementary Fig. 3**) when examined 4–8 d after plating. After 10 d of differentiation, however, cells with FL1$^+$ characteristics could no longer be detected in cultures derived from sorted FL1$^+$ cells, in contrast to matched FL1$^+$ samples cultured in stem cell conditions (**Fig. 1e**). The subsequent transfer of differentiated cultures into stem cell culture conditions did not reconstitute FL1$^+$ properties such as autofluorescence or sphere formation (**Fig. 1e**). Similarly, when we plated fresh glioma-derived cells in serum-rich conditions, the autofluorescent subpopulation and its spherogenic ability was irreversibly lost (**Supplementary Fig. 4**). The fact that FL1$^+$ cells were only present in stem cell culture conditions and were lost upon induction of differentiation suggests that FL1$^+$ cells may have properties similar to those of stem cells.

Self-renewal of FL1$^+$ cells

As self-renewal is a property of stemness in normal tissue and has also been used to characterize cancer stem cells[17], we tested the ability of FL1$^+$ cells to self renew in clonogenic assays. Single-cell plating of sorted FL1$^+$ and FL1^0 cells either from fresh dissociated glioma tissues or from glioma cell cultures revealed that FL1$^+$ cells have a superior capacity to self-renew than FL1^0 cells (**Fig. 2a**,**b**). We then measured the self-renewal ability of individual FL1$^+$ and FL1^0 clones over several successive cell passages. Whereas FL1$^+$ clones retained spherogenic potential for at least five passages,

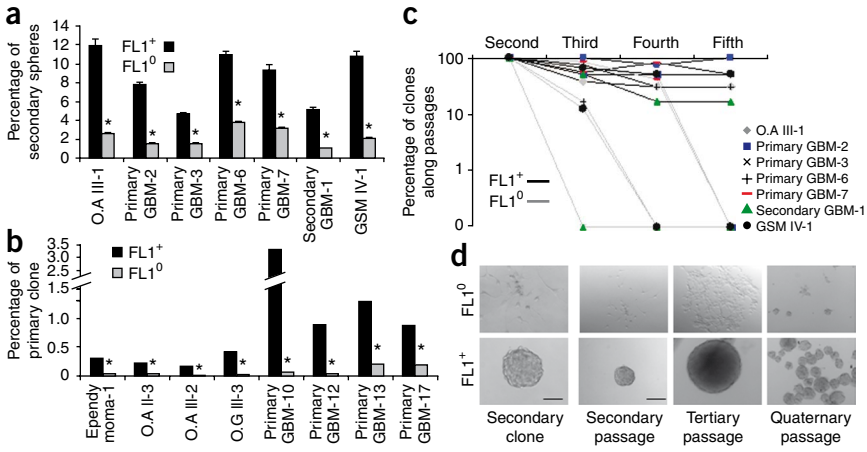

Figure 2 | FL1$^+$ cells display exclusive self-renewal abilities. (**a**) Quantification of single cells that form secondary spheres after sorting and clonal plating of FL1$^+$ and FL1^0 cells from the indicated samples. Errors bars, s.d. (n = 3); *P < 0.5. GBM, glioblastoma multiforme WHO grade IV; O.A III, oligoastrocytoma WHO grade III. (**b**) Quantification of single cells that form primary clones after isolation of FL1$^+$ and FL1^0 cells from the indicated samples. *P < 0.5. O.A II, oligoastrocytoma WHO grade II; O.G. III, oligodendroglioma WHO grade III. (**c**) Quantification of viable clones after serial passage (up to 5) of cells derived from a single FL1$^+$ or FL1^0 cell. (**d**) Phase-contrast images of an FL1$^+$ and an FL1^0 clone during serial passage. Scale bar, 50 μm (left) and 100 μm (right three panels).

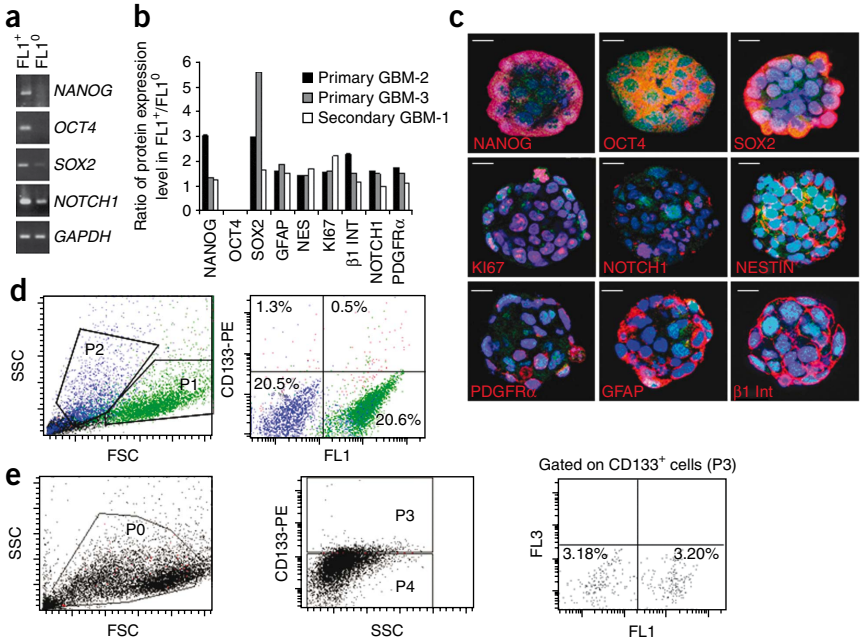

Figure 3 | Expression of stemness related genes in FL1$^+$ cells. (**a**) Representative reverse transcriptase (RT)-PCR analysis of gene expression in FL1$^+$ and FL1^0 cells. (**b**) The ratio of protein levels in FL1$^+$ cells versus FL1^0 cells is plotted for the indicated proteins, quantified by FACS. (**c**) Representative confocal images of primary glioblastoma multiforme (GBM)-3 gliomaspheres stained with the indicated stemness markers (red). Autofluorescence (green) and DAPI staining (blue) are also shown. Scale bar, 65 µm. (**d**) FACS analysis of cells dissociated from primary GBM-2 cell culture and stained for CD133 (left; gating is as in **Fig. 1a**) and expression of CD133 in the FL1$^+$ and FL1^0 cell populations (right). Red dots represent CD133$^+$ cells. Upper left, CD133$^+$ FL1^0; upper right, CD133$^+$ FL1^1; lower left, CD133$^-$ FL1^0; and lower right, CD133$^-$ FL1^1. Black dots represent the nongated population and percentages in each quadrant are relative to total viable cells. (**e**) FACS analysis of cells dissociated from primary GBM-2 cell culture and stained for CD133. Cells were gated on viable cells (P0; left). Expression of CD133 in viable glioma-initiating cells (P0) gated), P3 and P4 gate the CD133$^+$ and CD133$^-$ cell populations, respectively (middle). Distribution of the FL1$^+$ and FL1^0 cells from the CD133$^+$ cell population (P3) (right). Percentages in each quadrant are relative to total viable cells. FL3 channel: excitation at 556 nm and emission at 570 ± 15 nm as shown in **Supplementary Table 1**.

FL1^0 clones were lost between passage 3 and 4 with no clone capable of sustaining new sphere formation (**Fig. 2c** and **Supplementary Table 5**). FL1$^+$ spheres were larger, floating and apparently healthier than the partially attached and undersized FL1^0 clones (**Fig. 2d**). Moreover, FL1^0 derived clones did not contain any FL1$^+$ cells, whereas isolated FL1$^+$ cells could generate both FL1$^+$ and FL1^0 cells in passaged gliomaspheres (**Supplementary Fig. 5**).

Expression of stemness-related genes in FL1$^+$ cells

Several stem-cell and progenitor-cell gene expression profiles have been identified in gliomas or glioma-initiating cells[18–20]. To understand the molecular mechanisms underlying the selective stemness phenotype of FL1$^+$ glioma cells, we quantified the expression of 14 selected[18] stemness-related genes in FL1$^+$ and FL1^0 cells from four different gliomas. The only genes expressed more than twofold in FL1$^+$ cells were *NANOG*, *POU5F1* (also known as *OCT4*), *SOX2* and *NOTCH1* (**Fig. 3a** and **Supplementary Table 6**). FACS and confocal imaging analysis of stemness-related proteins corresponding to the above-mentioned genes revealed a preferential but not exclusive expression in FL1$^+$ cells (**Fig. 3b**,**c** and **Supplementary Fig. 6**). Although the majority of KI67$^+$ cells were confined to the FL1$^+$ cell fractions, FL1^0 cells also expressed KI67 (**Fig. 3b**,**c** and **Supplementary Fig. 6f**), suggesting that FL1^0 cells were viable and proliferated to some extent. We found a relatively low percentage of CD133$^+$ cells in both FL1^0 and FL1$^+$ cell compartments (**Fig. 3d**, **Supplementary Fig. 7** and **Supplementary Table 7**). Conversely, sorted CD133$^+$ cells were distributed in both FL1^0 and FL1$^+$ cell compartments (**Fig. 3e** and

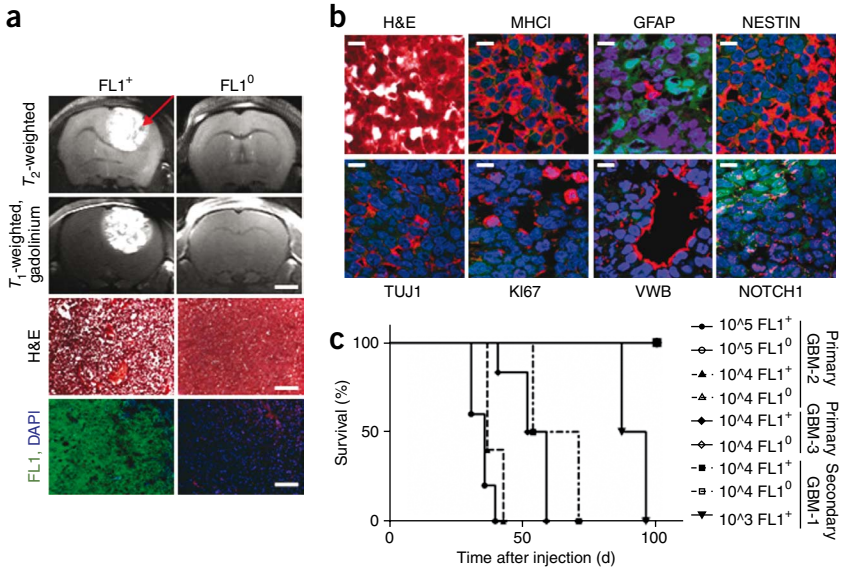

Figure 4 | FL1$^+$ cells initiate and sustain tumor growth *in vivo*. (**a**) Representative magnetic resonance images of mice brains after implantation with FL1$^+$ or FL1^0 cells from primary glioblastoma multiforme (GBM)-3 cell culture before (T_2-weighted fast-spin echo) and after contrast (T_1-weighted fast-spin echo with gadolinium contrast agent). Scale bar, 0.25 cm. Hematoxylin and eosin (H&E)-stained images and FL1 autofluorescent (green), DAPI-stained (blue) images of implanted brain slices are also shown; scale bars, 90 µm. (**b**) Fluorescence images of brain sections derived from FL1$^+$ implanted mice (primary GBM-3) and immunostained for the indicated markers (red). FL1 autofluorescence (green) and DAPI staining (blue) are also shown. Scale bars, 40 µm. (**c**) Analysis of mice after injection with different numbers of sorted FL1$^+$ and FL1^0 cells from the indicated samples.

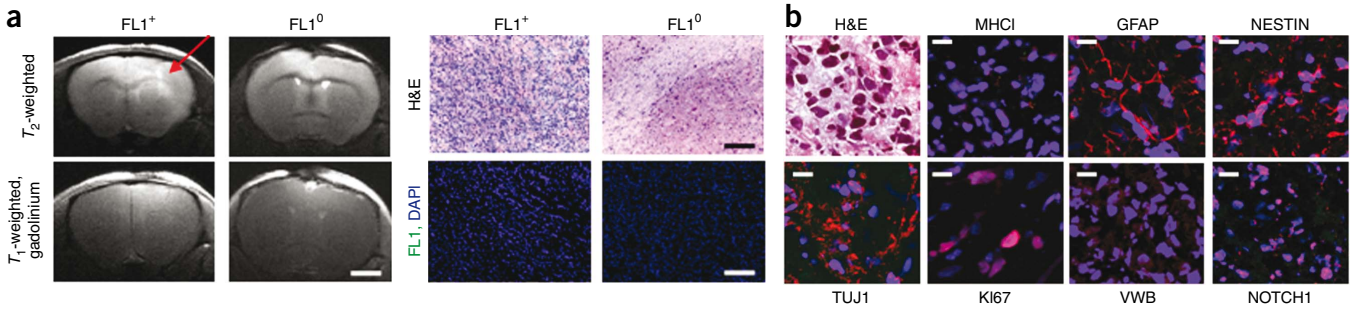

Figure 5 | Tumorigenic capacity of FL1$^+$ cells. (**a**) Representative magnetic resonance images of mice brains after implantation with FL1$^+$ or FL1^0 cells prospectively isolated from primary glioblastoma multiforme (GBM)-12, precontrast T_2-weighted fast-spin echo and postcontrast (T_1-weighted fast-spin echo with gadolinium contrast agent). Scale bar, 0.25 cm. Hematoxylin and eosin (H&E)-stained images and FL1 autofluorescent (green), DAPI-stained (blue) images of implanted brain slices are also shown; scale bars, 90 µm. (**b**) Fluorescence images of brain sections derived from FL1$^+$ cell–implanted mice (primary GBM-12) and immunostained for the indicated markers (red). FL1 autofluorescence (green) and DAPI staining (blue) are also shown. Scale bars, 40 µm.

Supplementary Table 8). Statistical analysis (paired *t*-test) of the percentage of FL1$^+$ cells and CD133$^+$ cells as determined by FACS in fresh primary glioblastoma multiforme ($P = 0.69$, $R^2 = 0.094$, $n = 4$) and gliomasphere cultures ($P = 0.58$, $R^2 = 0.094$, $n = 5$) confirmed that there was no correlation between the FL1$^+$ phenotype and the expression of CD133, suggesting that CD133 alone might not be sufficient to fractionate cancer-initiating and non-cancer-initiating cells.

FL1$^+$ cells were tumorigenic *in vivo*

To test whether glioma-initiating cells originated only from the FL1$^+$ population, we intracranially injected sorted FL1$^+$ or FL1^0 cells from fresh tissue or from two primary and one secondary glioblastoma multiforme–derived gliomasphere cultures (**Figs. 4** and **5** and **Supplementary Table 9**). When cells to be injected were isolated from gliomasphere cultures, all mice injected with FL1$^+$ cells, even with a load of 10^3 cells, exhibited substantial weight loss and neurological symptoms within few weeks, correlating with intracranial tumors observed on magnetic resonance images and histological sections (**Fig. 4** and **Supplementary Fig. 8**). We detected no tumors in FL1^0 cell–injected mice even at a 10^5 intracranial cell load after more than three months (**Supplementary Table 9**), except for one experiment, which subsequently revealed the presence of FL1$^+$ cells, potentially because of a residual contamination of FL1$^+$ cells during FACS. Upon injection of cells obtained from fresh glioma, only the mice implanted with the FL1$^+$ cells developed neurological symptoms by four months, which correlated with a massive infiltrative glioma (**Fig. 5**). Serial transplantation of freshly isolated FL1$^+$ cells confirmed that the tumorigenic potential was exclusively confined to the FL1$^+$ cell population (**Supplementary Table 10**). Implantation of as few as 3,000 FL1$^+$ cells was sufficient to initiate tumorigenesis within three months (data not shown). On histological sections, FL1$^+$ cell–induced tumors showed FL1 autofluorescence and contained a higher proportion of NESTIN$^+$ and KI67$^+$ cells compared to GFAP$^+$, TUJ1$^+$ cells (**Fig. 5b** and **Supplementary Fig. 8**). The human origin of the tumors was confirmed by human MHC-I staining (**Supplementary Fig. 9**). When we analyzed brains of injected mice after dissociation, we found FL1$^+$ cells only in FL1$^+$ cell–injected brains (**Supplementary Fig. 9**). Plating of dissociated cells resulted in the formation of many large spheres from FL1$^+$ tumors within 2 or 3 d, in contrast to cultures derived from FL1^0 cell–injected brains (**Supplementary Fig. 9**). These data suggest that a selection strategy based on phenotype can identify, in both glioma and glioma cultures, a subpopulation of glioma cells with exclusive *in vivo* tumorigenic potential.

DISCUSSION

Our data suggest that self-renewing and tumor-initiating glioma cells have a distinct morphology and autofluorescence, which allows their identification and isolation from non-tumorigenic glioma cells independently of CD133. FL1$^+$ cells were enriched for stemness-related genes, were multipotent, could generate FL1^0 cells and could self-renew over time (**Supplementary Fig. 10**). Moreover, as clonal gliomaspheres derived from FL1$^+$ cells contained a mixed population of FL1$^+$ and FL1^0 cells, FL1^0 cells should logically be derived from FL1$^+$ cells either by asymmetric division or by loss of properties associated with autofluorescence in some FL1$^+$ cells. Because FL1^0 cell–derived cultures did not yield any FL1$^+$ cells, FL1^0 cells may be committed tumor progenitors or differentiating cells that have lost their self-renewal and tumorigenic properties. We are currently studying the differentiation potential of FL1^0 cells. They are not cancer-initiating cells as they unambiguously do not have long-term self-renewal properties *in vitro* and are not tumorigenic *in vivo*. However, when plated under conditions that promote differentiation, FL1^0 cells expressed differentiation markers, as did FL1$^+$ cells under similar culture conditions. Thus the FL1^0 population may include progenitor cells in addition to more differentiated cancer cells.

We do not yet understand the molecular basis of the autofluorescence in FL1$^+$ cells. Several studies have linked autofluorescence with the cell cycle and/or cellular metabolic activity, such as the intracellular NAD/NADPH status or mitochondrial flavin content[21–23]. Our preliminary data suggest that autofluorescence in FL1$^+$ cells may reflect higher metabolic and proliferative activity (data not shown). In this respect, the relatively low autofluorescence levels and rarity of the FL1$^+$ population *in vivo*, relative to what we observed in *in vitro* culture, may indicate a more quiescent state of FL1$^+$ cells when growing in their natural tumor environment with lower oxygen levels, growth factor supply and glucose concentrations than those present *in vitro*.

Present knowledge of other normal and cancer tissues such as the hematopoietic system indicates that stem cells or early progenitor populations are rarely defined by only one but rather

by a combination of molecular markers[24]. Notably, none of the stemness genes (including CD133) that potentially could be used as a functional cancer stem cell marker, was exclusively restricted to the $FL1^+$ population as expression of all tested genes was also detectable in $FL1^0$ cells. Moreover, 'stemness', and in particular cancer stemness, might well be an elusive property that is not defined by invariable molecular markers but may have less stable molecular configurations that change with time and environmental context[12,13,25–27]. Differences between TICs and other tumor cells may not be as clear-cut as in normal tissues, in which a stringent hierarchy and strictly balanced asymmetric division guarantees tissue integrity[28,29]. As they are genetically altered, cancers might contain a spectrum of 'intermediate' tumor cells with various tumorigenic potencies and more or less aberrant differentiation states[3,26]. It may therefore be possible to consider cancer stemness in a given subpopulation or in single cells as a property with variable expressivity rather than a strictly committed on or off state with obligatory expression of defined markers.

Altogether, our data show that a subpopulation of glioma cells have an identifiable cellular phenotype strongly correlated with stemness and tumorigenic capacity and can be isolated without the use of molecular markers. Exploiting these properties may be more suitable to capture the dynamic complexity of tumor initiating cells and allow the identification of new therapeutic targets.

METHODS

Methods and any associated references are available in the online version of the paper at http://www.nature.com/naturemethods/.

Note: Supplementary information is available on the Nature Methods website.

ACKNOWLEDGMENTS

This work was supported by the foundations "Anita et Werner Damm-Etienne" and "Ernest and Lucie Schmidheiny" and in part by the Centre d'Imagerie Biomedicale of the Ecole Polytechnique Fédérale de Lausanne, the University of Lausanne, the University of Geneva and by the Leenaards and Jeantet foundations, as well as by Marie Curie action of the European Union (MRTN-CT-2006-035801) and the Swiss National Science Foundation (3100A0-108266/1). We thank K. Burkhardt for providing access to tissue sample collection and S.G. Clarkson for critical input.

AUTHOR CONTRIBUTIONS

I.R. and V.C. conceived the study and designed the experiments. V.C., D.M., M.-F.H., C.C. and V.M. performed all the experiments. I.R. and V.C. wrote the manuscript. P.-Y.D., M.E.H., R.G., N.d.T., V.C. and I.R. discussed, revised and checked the manuscript.

COMPETING INTERESTS STATEMENT

The authors declare competing financial interests: details accompany the full-text HTML version of the paper at http://www.nature.com/naturemethods/.

Published online at http://www.nature.com/naturemethods/.
Reprints and permissions information is available online at http://npg.nature.com/reprintsandpermissions/.

1. Wechsler-Reya, R. & Scott, M.P. The developmental biology of brain tumors. *Annu. Rev. Neurosci.* **24**, 385–428 (2001).
2. Read, T.A., Hegedus, B., Wechsler-Reya, R. & Gutmann, D.H. The neurobiology of neurooncology. *Ann. Neurol.* **60**, 3–11 (2006).
3. Sanai, N., Alvarez-Buylla, A. & Berger, M.S. Neural stem cells and the origin of gliomas. *N. Engl. J. Med.* **353**, 811–822 (2005).
4. Galli, R. *et al.* Isolation and characterization of tumorigenic, stem-like neural precursors from human glioblastoma. *Cancer Res.* **64**, 7011–7021 (2004).
5. Hemmati, H.D. *et al.* Cancerous stem cells can arise from pediatric brain tumors. *Proc. Natl. Acad. Sci. USA* **100**, 15178–15183 (2003).
6. Singh, S.K. *et al.* Identification of a cancer stem cell in human brain tumors. *Cancer Res.* **63**, 5821–5828 (2003).
7. Singh, S.K. *et al.* Identification of human brain tumour initiating cells. *Nature* **432**, 396–401 (2004).
8. Clement, V., Dutoit, V., Marino, D., Dietrich, P.Y. & Radovanovic, I. Limits of CD133 as a marker of glioma self-renewing cells. *Int. J. Cancer* **125**, 244–248 (2009).
9. Wang, J. *et al.* CD133 negative glioma cells form tumors in nude rats and give rise to CD133 positive cells. *Int. J. Cancer* **122**, 761–768 (2008).
10. Beier, D. *et al.* CD133(+) and CD133(–) glioblastoma-derived cancer stem cells show differential growth characteristics and molecular profiles. *Cancer Res.* **67**, 4010–4015 (2007).
11. Ogden, A.T. et al. Identification of A2B5+CD133– tumor-initiating cells in adult human gliomas. *Neurosurgery* **62**, 505–514 (2008).
12. Hill, R.P. Identifying cancer stem cells in solid tumors: case not proven. *Cancer Res.* **66**, 1891–1895 (2006).
13. Kern, S.E. & Shibata, D. The fuzzy math of solid tumor stem cells: a perspective. *Cancer Res.* **67**, 8985–8988 (2007).
14. Yuan, X. *et al.* Isolation of cancer stem cells from adult glioblastoma multiforme. *Oncogene* **23**, 9392–9400 (2004).
15. Piccirillo, S.G. *et al.* Bone morphogenetic proteins inhibit the tumorigenic potential of human brain tumour-initiating cells. *Nature* **444**, 761–765 (2006).
16. Park, D.M. *et al.* N-CoR pathway targeting induces glioblastoma derived cancer stem cell differentiation. *Cell Cycle* **6**, 467–470 (2007).
17. Reya, T., Morrison, S.J., Clarke, M.F. & Weissman, I.L. Stem cells, cancer, and cancer stem cells. *Nature* **414**, 105–111 (2001).
18. Clement, V., Sanchez, P., de Tribolet, N., Radovanovic, I. & Ruiz, I.A.A. HEDGEHOG-GLI1 signaling regulates human glioma growth, cancer stem cell self-renewal, and tumorigenicity. *Curr. Biol.* **17**, 165–172 (2007).
19. Gunther, H.S. *et al.* Glioblastoma-derived stem cell-enriched cultures form distinct subgroups according to molecular and phenotypic criteria. *Oncogene* **27**, 2897–2909 (2008).
20. Phillips, H.S. *et al.* Molecular subclasses of high-grade glioma predict prognosis, delineate a pattern of disease progression, and resemble stages in neurogenesis. *Cancer Cell* **9**, 157–173 (2006).
21. Kann, O., Schuchmann, S., Buchheim, K. & Heinemann, U. Coupling of neuronal activity and mitochondrial metabolism as revealed by NAD(P)H fluorescence signals in organotypic hippocampal slice cultures of the rat. *Neuroscience* **119**, 87–100 (2003).
22. Schuchmann, S., Kovacs, R., Kann, O., Heinemann, U. & Buchheim, K. Monitoring NAD(P)H autofluorescence to assess mitochondrial metabolic functions in rat hippocampal-entorhinal cortex slices. *Brain Res. Brain Res. Protoc.* **7**, 267–276 (2001).
23. Reyes, J.M. *et al.* Metabolic changes in mesenchymal stem cells in osteogenic medium measured by autofluorescence spectroscopy. *Stem Cells* **24**, 1213–1217 (2006).
24. Buzzeo, M.P., Scott, E.W. & Cogle, C.R. The hunt for cancer-initiating cells: a history stemming from leukemia. *Leukemia* **21**, 1619–1627 (2007).
25. Kaplan, R.N., Psaila, B. & Lyden, D. Niche-to-niche migration of bone-marrow-derived cells. *Trends Mol. Med.* **13**, 72–81 (2007).
26. Campbell, L.L. & Polyak, K. Breast tumor heterogeneity: cancer stem cells or clonal evolution? *Cell Cycle* **6**, 2332–2338 (2007).
27. Gilbertson, R.J. & Rich, J.N. Making a tumour's bed: glioblastoma stem cells and the vascular niche. *Nat. Rev. Cancer* **7**, 733–736 (2007).
28. Doetsch, F., Caille, I., Lim, D.A., Garcia-Verdugo, J.M. & Alvarez-Buylla, A. Subventricular zone astrocytes are neural stem cells in the adult mammalian brain. *Cell* **97**, 703–716 (1999).
29. Dontu, G., Al-Hajj, M., Abdallah, W.M., Clarke, M.F. & Wicha, M.S. Stem cells in normal breast development and breast cancer. *Cell Prolif.* **36** (Suppl. 1), 59–72 (2003).

ONLINE METHODS

Processing, clonogenic and differentiation assays on tumors and gliomasphere cultures. Primary brain tumors were obtained following approved institutional (HUG) protocols and written consent was obtained from all patients. Cells were cultured as in[4,8]. Media and growth factors were renewed once a week. Primary spheres are those spheres formed after fresh isolation of cells from tumors. Secondary spheres are the second generation of spheres generated from dissociated primary spheres. Sphere formation was assessed as reported[18] and presented as the percentage of clones derived from the initial number of cells plated. Self-renewal ability was monitored by dissociating spheres mechanically and transferring dissociated cells along successive passages as described previously[8]. Differentiation assays were performed as described previously[15].

FACS analysis of cells using morphology, autofluorescence and CD133 staining. Fresh glioma cells or dissociated cells from gliomaspheres cultures were adjusted at a concentration of 1 million cell per ml in 1× PBS (pH 7.4) before analysis or sorting either on Beckton Dickinson FACScan or FACSVantage or AriA (BD Bioscience). In gliomasphere cultures, $FL1^+$ cells were selected using the intersection of P1 and P4 and $FL1^0$ cells were selected using the intersection of P2 and P5 as shown in **Figure 1a**. For sorting from fresh glioma, the morphology and relatively low levels of fluorescence of the cells were taken into account for adjusting the gating by also incorporating cells with lower FL1 signal after selecting for appropriate morphology (low SSC and high FSC), that is, $FL1^+$ were selected using the intersection of P1 and P3 and $FL1^0$ were selected using the intersection of P2 and P5 (**Fig. 1c**). Characteristics of FL1 autofluorescence were evaluated by excitation with additional lasers at different wavelengths: 488 nm (Can, Vantage), 532 nm (Aria) 546 nm (Sorter), 632 nm (Calibur) (**Supplementary Table 1** and **Supplementary Fig. 1**). CD133 staining and expression level analyses were performed as described previsouly[8]. Cell viability was tested by addition of trypan blue (Sigma) at 1/1,000 dilution. FACS data analysis was performed using CellQuest and Diva software.

Statistical analyses. Paired *t*-test, correlation and linear regression were done using GraphPad Prism. Experiments were carried out in triplicate for each assay on each individual gliomasphere culture mentioned.

Antibodies. Mouse anti-KI67 (Chemicon Int.), goat anti-NOTCH1 (Santa Cruz), mouse anti-Integrinβ1 (Chemicon Int.), rabbit anti-PDGFRα (Spring Bioscience), mouse anti-MAP2 (Chemicon Int.), mouse anti-VWB (von willebrand, Dako), mouse anti-NESTIN (R&D systems), rabbit anti-GFAP (Sigma), goat anti-NANOG (R&D systems), mouse anti-SOX2 (R&D systems), rabbit anti-OCT4 (Abcam), mouse anti-TUJ1 (Covance), goat anti-NOTCH1 (Santa Cruz) mouse anti-HLA A-B-C (BD Pharmigen), anti-mouse Alexa Fluor 555–conjugated secondary antibodies (Molecular Probes), anti-goat-Cy3 (Jackson ImmunoResearch Laboratories) or Alexa Fluor 647–conjugated (Molecular Probes) and anti-rabbit-Cy3–conjugated (Jackson ImmunoResearch Laboratories). DAPI (Sigma) was only used to stain nucleus and was added with secondary antibodies.

Immunochemistry and confocal microscopy. Gliomaphere stainings were performed in suspension without any sphere dissociation. After fixation using 4% (wt/vol) PFA, gliomaspheres were incubated with 1× PBS with 1% (wt/vol) BSA and 0.1% (wt/vol) TritonX-100 for intracellular protein or without detergent for membrane receptor protein. Antibodies were diluted in 1× PBS with 1% BSA and incubated either overnight at 4 °C under rotation with primary antibodies or for 1 h at room temperature (20–22 °C) with secondary antibodies. For microscopy, gliomasphere were mounted between glass slide and coverslip before analysis on a LSM-510 Meta confocal microscope (Zeiss). For phase-contrast imaging on adherent and floating cultures, images were taken using the Openlab microscope (Zeiss). Image quantification and three-dimensional reconstruction were processed using the Imaris software, and quantified using the Metamorph software.

RNA extraction, RT-PCR and quantitative RT-PCR. Total RNAs were extracted using the RNAqueous-Micro kit (Ambion). Reverse transcription was performed using Superscript II (Invitrogen). Quantitative RT-PCR reactions were performed using the SYBR Green PCR master mix (Applied Biosystems) and samples were run on a 7900HT sequence detection system machine (Applied Biosystems). Primer sequences are available in ref. 18 and **Supplementary Table 11**. *GAPDH*, *TUBG1* and *EEF1A1* were used as control genes.

Mouse intracranial grafts and *in vivo* tumor imaging by MRI. Experimental procedures involving mice were approved by the Etat de Genève, Service Vétérinaire, authorization number 1007/3337/2. Mouse intracranial xenografts were performed as described previously[18]. The mice were anesthetized during the entire MRI experiment with isofluorane. The magnetic resonance images were acquired on an MRI System (Varian Scientific) interfaced to 14.1-Tesla magnet with a 26-cm horizontal bore (Magnex Scientific). A home-built 14 mm diameter two-loop quadrature coil was used both for radio frequencey (RF) excitation and signal reception. The MRI protocol involved a precontrast T_2-weighted fast-spin echo scan (a repetition time of 5 s, an effective echo time of 52 ms, a slice thickness of 0.6 mm, field of view = 24×24 mm^2, a 256^2 matrix size and eight echoes per scan) and a postcontrast T_1-weighted spin echo scan (a repetition time of 380 ms, an echo time of 17 ms and the same geometrical parameters) performed after intraperitoneal Gd administration (150 µl of Gadovist 1.0 which correspond to 5 µl of reagent per gram of weight).